

## RF Plasma Production and Heating Below Ion-Cyclotron Frequencies in Uragan Torsatrons

V.E. Moiseenko 1), V.L. Berezhnyj 1), V.N. Bondarenko 1), P.Ya. Burchenko 1), V.V. Chechkin 1), M.B. Dreval 1), I.E. Garkusha 1), L.I. Grigor'eva 1), D. Hartmann 2), R. Koch 3), V.G. Konovalov 1), V.D. Kotsubanov 1), Ye.D. Kramskoi 1), A.E. Kulaga 1), A.V. Lozin 1), A.I. Lysoivan 3), S.M. Maznichenko 1), V.K. Mironov 1), I.N. Mysiura 1) R.O. Pavlichenko 1), V.S. Romanov 1), A.N. Shapoval 1), A.I. Skibenko 1), A.S. Slavnyi 1), Yu.S. Stadnik 1), V.I. Tereshin 1), V.S. Voitsenya 1)

- 1) Institute of Plasma Physics NSC KIPT, Kharkiv, Ukraine
- 2) Max-Planck-Institut für Plasmaphysik, Greifswald, Germany
- 3) Laboratory for Plasma Physics - ERM/KMS, Brussels, Belgium

E-mail contact of main author: moiseenk@ipp.kharkov.ua

Key words: radio frequency experiments, impurity control, wall conditioning, torsatron.

**Abstract.** In IPP-Kharkiv there are two torsatrons (stellarators) in operation. The Alfvén resonance heating in a high  $k_{\parallel}$ -parallel regime is used on both machines. This method of heating is advantageous for small size devices since the heating can be accomplished at lower plasma densities than the minority and second harmonic heating. A series of experiments is performed aimed at study the features of the discharge with the THT (three-half-turn) antenna. Electron temperatures in the range  $\langle T_e \rangle \sim 0.2 - 0.5$  keV are achieved at the plasma densities  $\langle n_e \rangle \sim 0.5 \cdot 10^{13} - 1.5 \cdot 10^{13} \text{ cm}^{-3}$ . Plasma energy content is increased up to 5 times with respect to the plasma produced by the frame antenna prior to the THT antenna pulse. A new 4-strap shielded antenna is manufactured and installed in Uragan-2M.

A high frequency discharge for wall conditioning is introduced in Uragan-2M torsatron. The discharge is sustained by the specially designed small frame antenna. Rather efficient hydrogen dissociation is achieved in such conditions.

Self-consistent model is developed for simulations of plasma production with arbitrary ICRF antennas. It includes the system of the particle and energy balance equations for the electrons, ions and neutrals and the boundary problem for the Maxwell's equations. The Maxwell's equations are solved at each time moment for the current plasma density and temperature distributions. The Maxwell's equations solution allows determining a local value of the electron RF heating power, which influences on the ionization rate and, in this way, on the evolution of plasma density. First results of calculations of RF plasma production in the Uragan-2M stellarator with the frame-type antenna are presented.

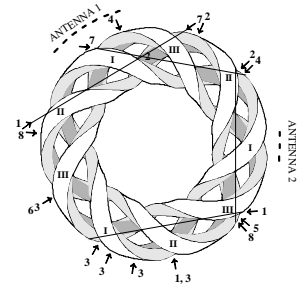
### 1. RF heating below ion-cyclotron frequencies in Uragan torsatrons

Uragan-3M is a small size torsatron with  $l = 3$ ,  $m = 9$ ,  $R_0 = 1$  m major radius,  $\bar{a} \approx 0.12$  m average plasma radius and toroidal magnetic field  $B_0 \leq 1$  T. The whole magnetic system is enclosed into a large 5 m diameter vacuum chamber. The Alfvén resonance heating in a high  $k_{\parallel}$  regime is used on this machine. This method of heating is advantageous for small size devices since the heating can be accomplished at lower plasma densities than the minority and second harmonic heating. Uragan-3M is equipped with two antennas. One is a frame-type antenna for low density plasma production. Another antenna in Uragan-3M is an unshielded THT (three-half-turn) antenna [1] that consists of 3 straps oriented in poloidal direction (*see FIG. 1*).

The strategy of usage of the Alfvén resonance heating with compact strap antenna (see e.g. [2]) is a result of balance of the technological restriction to have a compact antenna which occupies one device port and necessity to suppress the excitation of low  $k_{\parallel}$  Alfvén resonances that reside at the plasma periphery and cause plasma edge heating. The experiments with the THT antenna were attempted earlier [3, 4]. They showed increase of plasma density from  $\langle n_e \rangle \approx 0.5 \cdot 10^{12} - 2 \cdot 10^{12} \text{ cm}^{-3}$  provided by a pulse of the frame antenna to  $\langle n_e \rangle \sim 0.5 \cdot 10^{13} - 1.5 \cdot 10^{13} \text{ cm}^{-3}$ . In that time Uragan-3M was not equipped with a diagnostic for measuring the electron temperature. Since the expected heating in Alfvén resonance conditions is the electron heating, the result of those experiments remains incomplete. Second experiment also suffered from huge radiation losses that resulted in low plasma temperature what is indicated by the light emission from low charged states of light impurities. In current series of experiments, the electron cyclotron emission (ECE) diagnostics is employed. On-axis magnetic field value is  $B_0 = 0.72 \text{ T}$ . For this magnetic field the cut-off value of plasma density is  $\langle n_e \rangle \sim 0.85 \cdot 10^{13} \text{ cm}^{-3}$ . This value is limiting for ECE diagnostics. Taking into account this fact, the experimental series is organized so that this level would be not exceeded despite the higher levels of plasma densities are achievable.



FIG. 1. THT antenna.



- 1 - optic spectroscopy
- 2 - microwave reflectometry and interferometry
- 3 - probe measurements
- 4 - ECE
- 5 - laser impurity injection
- 6 - SXR
- 7 - CX neutral energy analyzers
- 8 - magnetic diagnostics

FIG. 2. Scheme of Uragan-3M diagnostics.

The diagnostics involved into these experiments are shown on Fig. 2. The frequency of heating is chosen so, that the peaking  $k_{\parallel}$  value in the antenna spectrum satisfy the Alfvén resonance condition at the plasma core. Since the device is small and  $k_{\parallel}$  is high the frequency should be chosen quite close to the ion cyclotron. It is  $f_1 = 8.6 \text{ MHz}$  for the frame antenna and  $f_2 = 8.9 \text{ MHz}$  for the THT antenna. For these frequencies the ion cyclotron zone is present in plasma column. In regular discharges the frame antenna creates plasma with the density  $\langle n_e \rangle \sim 0.5 \cdot 10^{12} - 2 \cdot 10^{12} \text{ cm}^{-3}$  and temperature  $\langle T_e \rangle \sim 1 \text{ keV}$ . In the experiments the pulse of the frame antenna goes first. Immediately after the frame antenna pulse the THT antenna is switched on. The temporal evolution of the plasma parameters in such a shot is shown in Fig. 3.

The frame antenna ionizes the neutral gas during 1-4 ms and heats low-density plasma. The power delivered to the antennas is about  $P_1 \sim 100 \text{ kW}$  for the frame antenna and  $P_2 \sim 150 \text{ kW}$  for the THT antenna. Plasma density is  $\langle n_e \rangle \sim 10^{12} \text{ cm}^{-3}$  during the frame

antenna pulse. After it the plasma density grows rapidly to  $\langle n_e \rangle \sim 2.5 \cdot 10^{12} \text{ cm}^{-3}$  and, further is ramping up to  $\langle n_e \rangle \sim 3.5 \cdot 10^{12} \text{ cm}^{-3}$  at the end of the THT antenna pulse. Carbon CV line emission is higher during the THT antenna pulse. CIII line emission is small during the whole shot, but there is a huge recombination peak after the THT antenna pulse indicating that carbon is in highly ionized states in the plasma. Electron temperature is calculated from the radiation temperature by  $T_e = T_{rad} / (1 - e^{-\tau})$  by means of tokamak approximation formula for the optical thickness of the plasma  $\tau \approx 5.6 \cdot 10^{-14} \frac{\langle n_e \rangle T_e R_0}{B_0}$  [5] (here the plasma density is in  $\text{cm}^{-3}$ , electron temperature is in eV, torus major radius  $R_0$  is in cm, and the magnetic field is in G).

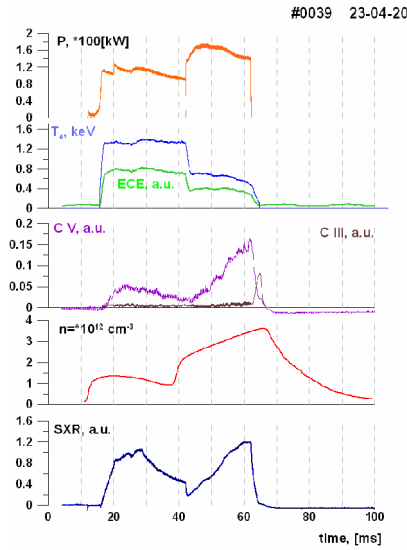


FIG. 3. Evolution of RF power, radiation and electron temperature, CV and CIII lines emission, plasma density and SXR intensity in a shot with continuous gas puff. Neutral gas pressure is  $9.3 \cdot 10^{-6}$  Torr .

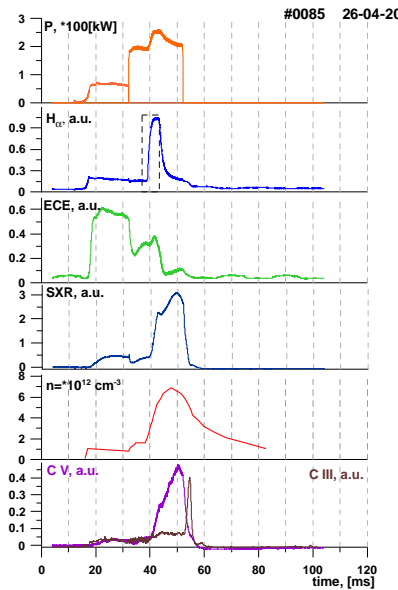


FIG. 4. Evolution of RF power,  $H\alpha$  hydrogen line intensity, ECE signal, soft x-ray intensity, plasma density and CV and CIII lines emission in a shot with a strong pulsed gas puff. Neutral gas pressure is  $9.3 \cdot 10^{-6}$  Torr .

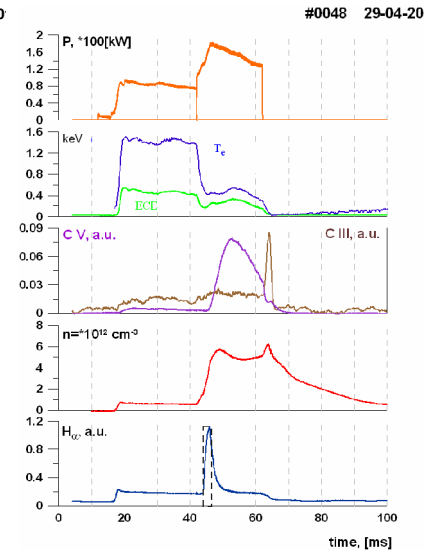


FIG. 5. Evolution of RF power, radiation and electron temperature, CV and CIII lines emission, plasma density and  $H\alpha$  hydrogen line intensity in a shot with a moderate pulsed gas puff. Neutral gas pressure is  $4.9 \cdot 10^{-6}$  Torr .

During THT antenna pulse electron temperature is lower, but the electron energy content is almost the same as compared with the frame antenna plasma. It is difficult to increase plasma density with continuous gas puff. For this purpose a pulsed gas puff is used. An example of a pulse with gas puff is given in Fig. 4. The gas puff causes a splash on  $H\alpha$  hydrogen spectral line emission. The plasma density, soft x-ray and CV emission signals grow substantially. The ECE signal also starts to grow at the beginning of the gas puff pulse, but then decreases. This behaviour could be explained by locking of ECE emission in dense plasma. Soft x-ray diagnostics and CV radiation intensity indicate that plasma is not cold. The plasma density comes close to the value  $\langle n_e \rangle \sim 8 \cdot 10^{12} \text{ cm}^{-3}$  demonstrating the THT antenna ability to increase plasma density to such values.

With more powerful gas puff the plasma density could be further increased, but the diagnostics indicate decrease of the plasma energy content. Tuning the gas puff intensity, the maximum plasma density is decreased to values  $\langle n_e \rangle \sim 5 \cdot 10^{12} - 7 \cdot 10^{12} \text{ cm}^{-3}$  that allows one to enable electron temperature measurements. One of such pulses is shown in Fig. 5. In this pulse during THT operation the density is  $\langle n_e \rangle \sim 5 \cdot 10^{12} \text{ cm}^{-3}$  and the electron temperature  $T_e = 0.5 \text{ keV}$  is achieved in the plasma column centre. The specific feature of plasma density behaviour is that after the gas puff the density does not return to the value which was before gas puff. The radial distribution of the CV intensity is calculated pulse by pulse chord measurements (Fig. 6). It is central at both stages of the discharge. The  $\text{C}^{4+}$  ion temperature is measured using Doppler spectrometry of a CV line. The estimates for Coulomb ion-ion collisions gives fast energy exchange between protons and  $\text{C}^{4+}$  ions. Thus their temperatures should be close to each other. The ion temperature is smaller than the electron one. It ramps up continuously during the THT antenna pulse and reaches the values close to  $T_i = 100 \text{ eV}$  by the pulse end.

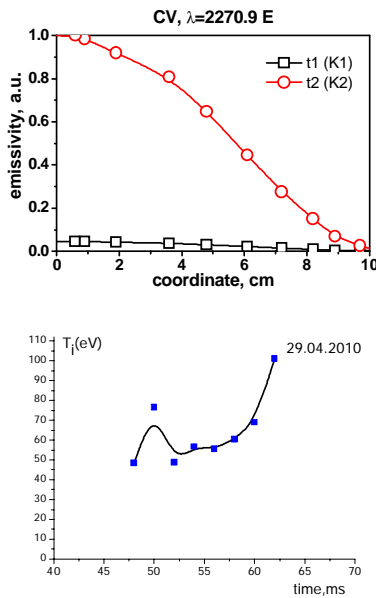


FIG. 6 (upper). Radial distributions of  $\text{C}^{4+}$  spectral line emissivity at time moments  $t_1 = 19 \text{ ms}$  (black) and  $t_2 = 50 \text{ ms}$  (red).

FIG. 7 (lower). Evolution of  $\text{C}^{4+}$  ion temperature in moderate pulsed gas puff shots.

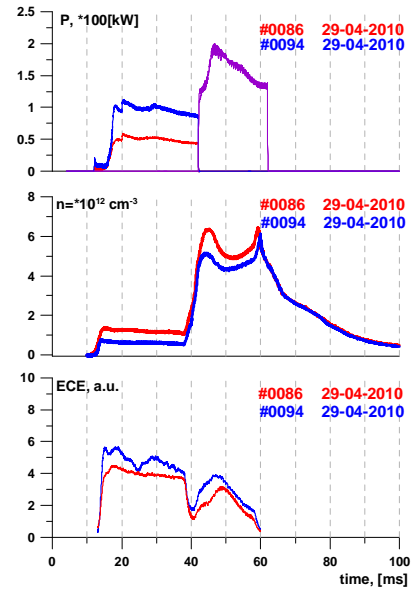


FIG. 8. RF power, plasma density and ECE intensity in two shots with different power delivered to the frame antenna.

The influence of frame antenna discharge on the THT antenna pulse is illustrated in comparison of two shots with different power delivered to the frame antenna (Fig. 8).

Decrease of power results in some increase of plasma density throughout the shot and connected to this small decrease of plasma electron temperature.

## 2. Wall conditioning discharges in Uragan-2M

At Uragan-2M torsatron (stellarator) the studies of the RF discharges for wall conditioning have been carried out. The machine has the major plasma radius  $R = 1.7 \text{ m}$ , the average minor plasma radius  $\bar{a} = 0.22 \text{ m}$  and the toroidal magnetic field  $B_0 \leq 2.4 \text{ T}$ . The goal of

the discharge wall conditioning is the removal of adsorbed species from the wall so that they may then be pumped out of the vacuum chamber. The adsorbed atoms or molecules may be removed by the ion or atom impact owing to the momentum transfer or chemical interaction. If during the wall conditioning plasma is magnetically confined, as would happen in superconducting stellarators, the outflow of ions is not intensive and their flux to the wall of the vacuum vessel is not uniformly distributed. Under such conditions, the wall conditioning with chemically active neutral atoms or molecules [6] is advantageous. Such neutrals are produced intensively from a molecular gas in partially ionized plasma when the degree of ionization is low. Such a scenario for wall conditioning is studied for the discharges in hydrogen. In this scenario the cleaning agents are the hydrogen atoms resulting from the dissociation of the hydrogen molecules. They have Franck-Condon energies, about 3 eV. If the electron temperature in the discharge is less than the ionization threshold, 4-10 eV, the dissociation rate is higher than the ionization, and one electron produces a number of neutral atoms during its lifetime.



FIG. 9. Frame antenna inside vacuum vessel.

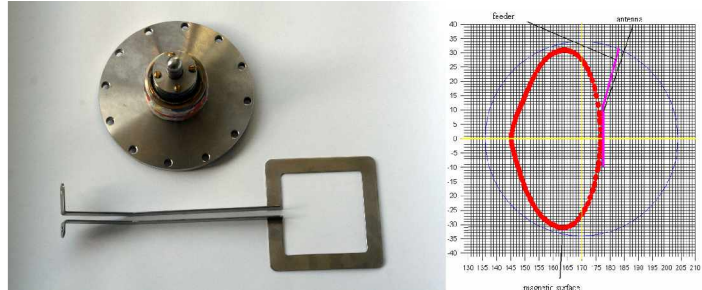


FIG. 10. Small frame antenna for wall conditioning (left) and its position with respect of the last closed magnetic surface (right).

The cleaning discharges could be continuous or pulsed. In continuous discharges the plasma density is low  $n_e = 10^8 - 10^{11} \text{ cm}^{-3}$ . Such a low density discharge could be sustained by excitation of the slow wave. This wave could be excited by any antenna having currents parallel to the steady magnetic field [7]. The frame antenna is the most simple antenna having such ability.

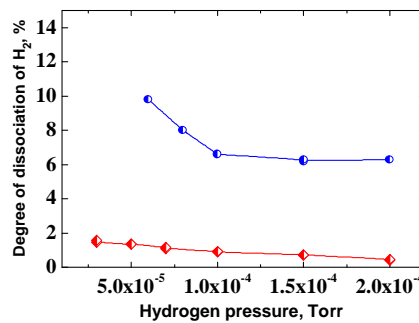


FIG. 11. Dissociation degree of hydrogen in low ( $f = 8.4 \text{ MHz}$ , red curve) and high ( $f = 135 \text{ MHz}$ , blue curve) frequency discharges.

The dispersion equation for the wave is the following  $k_{\perp}^2 = -\frac{\epsilon_{\parallel}}{\epsilon_{\perp}}(k_{\parallel}^2 - k_0^2 \epsilon_{\perp})$ , where  $\epsilon_{\perp} = \mathbf{E} \times \mathbf{B} \cdot \mathbf{\epsilon} \mathbf{E} \times \mathbf{B} / (EB)^2$ ,  $\epsilon_{\parallel} = \mathbf{B} \cdot \mathbf{\epsilon} \mathbf{B} / B^2$  are the perpendicular and parallel dielectric

tensor components,  $k_0 = \omega/c$ . If the frequency of the wave is higher than ion cyclotron the wave propagates if  $\varepsilon_{\perp} > 0$ . This requirement imposes an upper limit for plasma density.

In the first experimental series the continuous RF discharges in Uragan-2M torsatron are sustained by the 1 kW RF oscillator in the frequency range 4.5-8.8 MHz [8]. This power is coupled to plasma by a frame antenna (Fig. 9). Because of the above mentioned plasma density limitation, plasma with low density up to  $n_e = 8 \cdot 10^9 \text{ cm}^{-3}$  is sustained. The dissociation degree of hydrogen given by the optical measurements [8] for such a discharge is displayed in Fig. 11. The dissociation degree is not high. To increase it, higher plasma density is necessary. To achieve higher discharge performance, a higher frequency RF heating at 135 MHz is chosen. A new small frame antenna (Fig. 10) is manufactured and installed in Uragan-2M. This antenna shows better results in dissociation of hydrogen (Fig. 11).

### 3. Self-consistent model of the RF plasma production in stellarator

#### 3.1. Numerical model

The model of the radio-frequency (RF) plasma production includes the system of the balance equations and the boundary problem for the Maxwell's equations. It is assumed that the gas in atomic hydrogen. The system of the balance equations of particles and energy reads:

$$\frac{3}{2} \frac{\partial(k_B n_e T_e)}{\partial t} = P_{RFe} - \frac{3}{4} k_B \varepsilon_H \langle \sigma_e v \rangle n_e n_a - (C_a + 1) \frac{k_B n_e T_e}{\tau_E} - k_B \varepsilon_H \langle \sigma_i v \rangle n_e n_a + \nabla \cdot \chi \nabla (n_e T_e),$$

$$\frac{dn_e}{dt} = \langle \sigma_i v \rangle n_e n_a - \frac{n_e}{\tau_E} + \nabla \cdot D \nabla n_e, \quad (1)$$

$$\int n_e dV + n_a V_V = n_0 V_V = \text{const},$$

where  $n_e$  is the plasma density,  $n_a$  is the neutral gas density,  $T_e$  is the electron temperature,  $P_{RFe}$  is the RF power density, which is delivered to electrons,  $k_B$  is the Boltzman's constant,  $\varepsilon_H = 13.6 \text{ eV}$  is the ionization threshold for hydrogen atom,  $\chi$  is the heat transport coefficient,  $D$  is the diffusion coefficient,  $\tau_E$  is the particle confinement time,  $V_V$  is the vacuum chamber volume,  $\langle \sigma_e v \rangle$ ,  $\langle \sigma_i v \rangle$  are the excitation and ionization rates and  $C_a = e\Phi_a / T_e \approx 3.5$  is the ratio of the ambipolar potential energy to the electron temperature.

The balance of the electron energy includes the RF heating, energy losses for the excitation and ionization of atoms and losses caused by the heat transport. The balance of the charged particles includes accounts for the ionization and diffusion losses of particles. The last equation in system (1) reflects the global balance of the particles. It is assumed, that the neutral gas is uniformly distributed in the vacuum chamber volume, including the plasma column.

Apart from plasma inside the confinement volume, the RF field can produce plasma outside it. The losses of the charged particles in this region have a convection character: the particles escape to the wall along lines of force of the magnetic field. Such losses of particles outside the confinement volume are described in  $\tau$ -approximation.

The problem is solved in cylindrical geometry. The plasma is assumed to be azimuthally symmetrical and uniformly distributed along plasma column. The length of plasma cylinder is  $L = 2\pi R$  and the ends are assumed to be identical.

To make the system of the equations (1) closed it is necessary to determine the single external quantity in it,  $P_{RFe}$  (RF power density). This quantity can be found from the solution of the boundary problem for the Maxwell's equations:

$$\nabla \times \nabla \times \mathbf{E} - \frac{\omega^2}{c^2} \boldsymbol{\epsilon}(r) \cdot \mathbf{E} = i\omega\mu_0 \mathbf{j}_{ext} \quad , \quad (2)$$

)

where  $\mathbf{E}$  is the electric field,  $\mathbf{j}_{ext}$  is the external RF currents,  $\boldsymbol{\epsilon}$  is the dielectric tensor.

The Maxwell's equations are solved at each time moment for current plasma density and temperature distributions. The Maxwell's equations solution allows determining the value of local RF heating power of the electron plasma component which influences on the ionization rate and, in this way, on the increase of plasma density.

The Crank-Nicholson method is used for the solving of system of the balance equations (1). The Maxwell's equations (2) are solved in 1D using the Fourier series in the azimuthal and the longitudinal coordinates. For the discretization in radial coordinate, the uniform finite elements method is employed that uses a special set of weight (test) and basis (shape) functions [10].

### 3.2. Example of calculations

The following parameters of calculations for Uragan-2M stellarator are chosen: the major radius of the torus is  $R = 1.7 \cdot 10^2 \text{ cm}$ , the radius of the plasma column is  $r = 22 \text{ cm}$ , the radius of the metallic wall is  $a = 34 \text{ cm}$ , the radial coordinate of the antenna is  $l_r = 23 \text{ cm}$ , the toroidal magnetic field is  $B = 5 \text{ kG}$ , the antenna size of the frame antenna of azimuthal angle is  $\varphi_a = 1$ , the angular size of the frame antenna in the toroidal direction  $\vartheta_a = 0.08$ . The current in antenna is assumed not varying along the conductors.

The first results of calculations of RF plasma production in the Uragan-2M stellarator are presented. *Figs. 12, 13* display the profiles of the plasma density and the electron temperature at the time moment  $t = 0.02 \text{ s}$ . *Figs. 14-16* display the time evolution of the plasma density, density of neutral gas and the electron temperature.

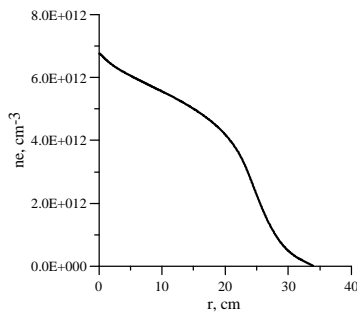


FIG.12. Profile of plasma density in  $t = 0.02 \text{ s}$ .

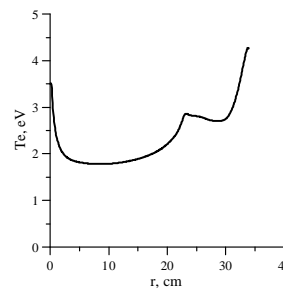


FIG. 13. Profile of electron temperature in  $t = 0.02 \text{ s}$ .

A characteristic feature of the calculations is sufficiently high plasma temperature outside the confinement volume (*Fig. 13*). Since the heating power per particle is high at lower plasma densities (*Fig. 12*) the electron temperature is increased at the edge of the plasma column (*Fig. 13*) where the particle losses are faster. For the reason that the slow wave is focused at the center of the plasma column, the peak of electron temperature is observed at this region (*Fig. 13*).

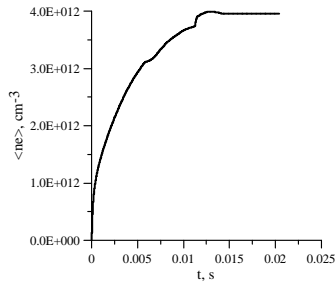


FIG. 14. Time evolution of average plasma density.

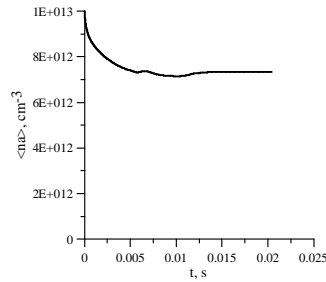


FIG. 15. Time evolution of average neutral atoms density.

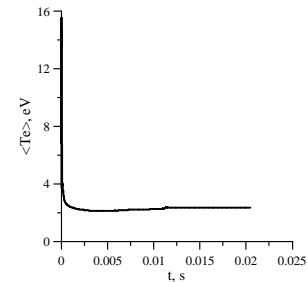


FIG.16. Time evolution of average electron temperature.

In the chosen regime the plasma density is ceased to increase and the plasma production process stagnates because the power is insufficient to complete burnout of neutral atoms (*Figs. 14, 15*).

At the initial stage of the plasma production sharp peaks in temperature are observed (*Fig. 16*). These peaks are associated with a sharp increase of the antenna loading resistance. It occurs when the wave global resonance conditions in a plasma column is met. At the initial stage of plasma production a slow wave damping is small, and the peaks of the global resonances are more narrow and high.

## Acknowledgement

This work is supported in part by STCU project № 4216. Authors are thankful to the technical staff of stellarators department for assistance in the experiments.

## References

- [1] Moiseenko, V.E. in IAEA Technical Committee Meeting (Proc. 8th Int.Workshop on Stellarators, Kharkov 1991), IAEA, Vienna (1991) 207.
- [2] Moiseenko, V.E., et al., Plasma Physics Reports 35(2009) 828.
- [3] Lysoivan, A.I., et al., Fusion Engineering and Design 26 (1995) 185.
- [4] Burchenko, P.Ya., et al., Visnyk KhNU, Ser. Phys. 2 (18), №559 (2002) 52 (in Russian).
- [5] Bornatici, M., et al., Nucl. Fusion 23 (1983) 1153.
- [6] Winter, J., Plasma Phys. Control. Fusion 38 (1996) 1503.
- [7] Moiseenko, V.E. Transactions of Fusion Technology 39 (2001) 65.
- [8] Moiseenko, V.E., et al., “Wall conditioning RF discharges in Uragan-2M torsatron”, 36th EPS Conference on Plasma Phys. Sofia, June 29 - July 3, 2009 ECA Vol.33E, P-5.199 (2009).
- [9] Lysojvan, A.I., et al., Nuclear Fusion 32 (1992) 1361.
- [10] Moiseenko, V.E., et al., Problems of Atomic Science and Technology, Series Plasma Physics (7), 4 (2002) 100.